MedChemComm

Accepted Manuscript

This is an *Accepted Manuscript*, which has been through the Royal Society of Chemistry peer review process and has been accepted for publication.

Accepted Manuscripts are published online shortly after acceptance, before technical editing, formatting and proof reading. Using this free service, authors can make their results available to the community, in citable form, before we publish the edited article. We will replace this *Accepted Manuscript* with the edited and formatted *Advance Article* as soon as it is available.

You can find more information about *Accepted Manuscripts* in the Information for Authors.

Please note that technical editing may introduce minor changes to the text and/or graphics, which may alter content. The journal's standard Terms & Conditions and the Ethical guidelines still apply. In no event shall the Royal Society of Chemistry be held responsible for any errors or omissions in this *Accepted Manuscript* or any consequences arising from the use of any information it contains.

ROYAL SOCIETY OF CHEMISTRY

www.rsc.org/medchemcomm

MedChemComm

ARTICLE

Insight into the selective inhibition of JNK family members through structure-based drug design†

Received 00th January 20xx,
Accepted 00th January 20xx

DOI: 10.1039/x0xx00000x

www.rsc.org/

A. Messoussi [a,b], G. Chevé [a], K. Bougrin[b]*, A. Yasri [a]*

The c-Jun N-terminal kinase (JNK) family, which comprises JNK1, JNK2 and JNK3, belongs to the mitogen-activated protein kinase (MAPK) super family, whose members regulate myriad biological processes, including ones implicated in tumorigenesis and neurodegenerative disorders. As many other kinases, JNKs can adopt two main conformational changes: the *DFG-in* (active) conformation and the *DFG-out* (inactive) conformation; however, to date, the only resolved DFG-out conformation is that of JNK2. Structural elucidation of the remaining DFG-out conformations will be critical for structure-based drug design of novel type-II inhibitors, which have been shown to offer greater therapeutic benefit than do type-I inhibitors, as demonstrated by Imatinib in chronic myeloid leukemia. Herein we report use of a homology-modeling approach to build models of the DFG-out conformations of JNK1 and JNK3. After validating the model structures, we used structure-based drug design to elucidate the principal structural differences among the three JNK active sites and the binding of known JNK inhibitors, and to explain the selectivity of these compounds for JNK2. Our findings provide structural guidelines for the design of novel and selective type-II JNK inhibitors.

Introduction

Kinases as therapeutic targets

Kinases are the largest family of enzymes encoded by the human genome. They transfer signals throughout the cell by catalyzing substrate phosphorylation in their highly conserved ATP binding sites.[1] Thus, each kinase, in its active site, transfers a phosphoryl group from an ATP molecule to its substrate (*e.g.* another protein, a lipid or a nucleic acid).

Over the past few decades, kinases have emerged as among the most desirable targets for drug discovery.[2] This is due to their ubiquity in cell-signaling pathways, the ease of assay development and analysis for kinases relative to other targets (*e.g.* proteases, transporters and voltage-gated ion channels), and to the inherent druggability and the success of kinase inhibitor drugs already on the market (*e.g.* Tarceva, Sutent and Gleevec).[3]

[a] OriBase Pharma, Parc Euromedecine, Cap Gamma, 1682, rue de la Valsière, CS17383, 34189 Montpellier cedex 4 – France. E-Mails: ayasri@oribase-pharma.com. Tel : +33 (0)4 67 727 670. FAX : +33 (0)4 67 727 679.
[b] Laboratoire de Chimie des Plantes et de Synthèse Organique et Bioorganique, URAC23, Université Mohammed V, Faculté des Sciences B.P., 1014 Rabat, Morocco. E-Mail: khalid.bougrin@smct-ma.com
† The authors declare no competing interests.

MAP kinases and the JNK family

C-Jun N-terminal kinases (JNKs) belong to the mitogen-activated protein (MAP) kinase super family. The JNK family comprises three members (JNK1, JNK2, and JNK3), which exist in a total of ten isoforms[4] and which are encoded by three separate genes (*Mapk8*, *Mapk9* and *Mapk10*, respectively).[5] These three JNKs differ by tissue distribution: JNK1 and JNK2 are ubiquitously expressed in organisms, whereas JNK3 is expressed mainly in the nervous system, in cardiac muscle and in the testes.[6–9]

JNKs are involved in one of three distinct MAPK pathways identified in mammalian cells. They are activated by extracellular stress factors such as cytokines, fatty acids, UV irradiation, heat shock and osmotic shock.[10,11] Originally, the first identified transcription factor specifically phosphorylated by JNKs was the C-jun, that why they were named the C-jun N-terminal kinase, but recent studies have shown that they phosphorylates and regulates also the activity of other transcription factors as ATF2, Elk-1, p53 and c-Myc[4,12–14] and non-transcription factors, such as members of the Bcl-2 family (Bcl-2, Bcl-xL, Bim and BAD).[15–17] Until today the investigations published about JNK pathways conclude that it is still complicated to clearly differentiate between the upstream phosphorylation of each JNK isoform and their specific function also. Although there are many JNK substrates, it is still a challenge to identify the molecular networks regulated by the individual JNK family members[18]. In spite of this, some isoforms preferences against a particular substrate

were observed, such as JNK2 which shows a preferential interaction with the substrate DCX protein, rather than JNK1,[19] or JNK1 which is more effective against the ligase Itch than JNK2.[20]

JNK implication in pathologies

Given their distinct expression patterns, JNKs are involved in diverse physiological and pathological processes, including ones that can lead to apoptosis and to mitogenic or proinflammatory signals.[11,21] Animal models of human disease, and clinical studies, have imputed JNKs in Alzheimer's disease[22], arthritis[23,24], asthma[25–27], atherogenesis[28], tumorigenesis[29], type I and type II diabetes[29,30,31], heart failure [32] and Parkinson's disease.[33,34]

In the work reported here, we studied the JNK kinase domains—particularly, the DFG-out (inactive) conformation of each enzyme. We sought to identify the structural elements implicated in the interactions between each JNK and its inhibitors, and to determine the differences among the three JNK active sites. We envisaged that such knowledge would ultimately prove useful for the design and development of type II selective inhibitors for each JNK conformation.

Materials and methods

Data sources

The three-dimensional structure of JNK2 (PDB IDs: 3NPC and 3E7O) was retrieved from the Protein Data Bank.[35] The primary sequences of JNK1 and JNK3 were retrieved from the UniProt database (Uniprot ID: P45983 and P53779, respectively).[36]

Homology modelling

Sequence alignment was performed using CLUSTAL O (1.2.1)[37], a multiple sequence alignment application from the Align tool of UniProt. SWISS-MODEL server[38,39] was used to build the homology models of JNK1 and JNK3 in their DFG-out conformations, using the X-ray structure of JNK2 DFG-out as a template. The obtained models were structurally validated using Procheck software.[40] In a SWISS-MODEL session, the JNK1 sequence was uploaded in the target space. For the template, the PDB X-ray structure 3NPC[41], containing two JNK2 chains (A and B) co-crystallized with Birb796 (a small organic molecule kinase inhibitor) (Figure 5a), was selected. Chain A was isolated as a PDB file by PyMOL and uploaded as a template in SWISS-MODEL. The JNK1 and JNK3 DFG-out 3D-models were built using SWISS-MODEL online software.

Docking

Autodock Vina software[42] was used to perform the docking calculations, using the default settings. For the DFG-out conformation, the grid box dimensions were defined as 20 Å (x), 29 Å (y) and 17 Å (z). The results were obtained as a pdbqt file and were visualized using PyMOL software.[43]

Results and discussion

Structural description of kinases

Kinases exhibit a highly conserved tertiary structure characterized by two separate lobes: the N-terminal lobe (N-ter) and the C-terminal lobe (C-ter). The space formed between these two lobes is obstructed by the labile activation loop (A-loop), which can close the lateral open side of this pocket to define the kinase active site or ATP binding site. The flexibility of this loop enables each kinase to adopt two catalytically important conformations (Figure 1). The *active conformation*, in which the substrate can bind, is called the *DFG-in conformation*, because the side chain of the Phe residue of the DFG (Asp-Phe-Glu) triplet in the activation loop points towards the inside of the active site. The *inactive conformation*, which prevents the substrate from binding to the kinase domain, is known as the DFG-out conformation, as the aforementioned side chain points towards the outside of the active site. Interestingly, both conformations are being targeted in drug design. Inhibitors that bind to the active site of a kinase in its DFG-in conformation and form non-covalent interactions with the surrounding residues are known as type-I kinase inhibitors, whereas those that bind to the DFG-out conformation are known as type-II kinase inhibitor.

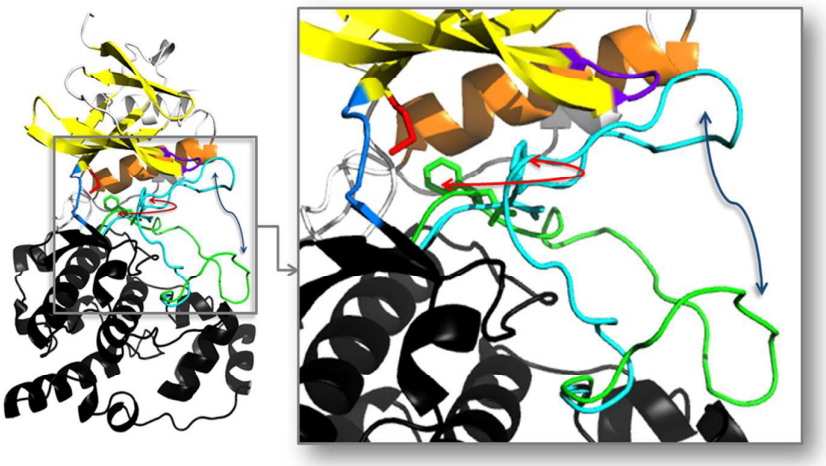

Figure 1 Alignment of the JNK2 DFG-in (PDB ID: 3E7O) and DFG-out (PDB ID: 3NPC) conformations. The co-crystalized ligand Birb769 in the DFG-out conformation is highlighted in cyan. The blue arrow signals the displacement of the activation A-loop, and the red arrow indicates the positioning of the Phe residue of the DFG triplet within the active site.

Homology modeling

Construction of the JNK1 and JNK3 models. In order to begin model construction, we required the 3D structures of JNK1, JNK2 and JNK3. At the time of writing, the following 3D crystallized JNK structures were available in the PDB database: the DFG-in conformations of each JNK, and the DFG-out conformation of JNK2 only; to date, no 3D crystallized DFG-out structures have been published for JNK1 or JNK3. Furthermore, the only available 3D-structure of JNK2 in its DFG-out conformation represents co-crystallization of this kinase with the MAPK inhibitor Doramapimod (BIRB796, PDB ID: 3NPC)[41](Figure 5b). Thus, our first task was to elucidate the DFG-out 3D-structures for JNK1 and the JNK3.

Thus, we based our homology modeling on three facts. Firstly, that proteins whose sequence homology is greater than 20% exhibit similar tertiary structures.[44,45] Secondly, that evolutionarily related proteins exhibit very similar 3D-structures.[46] Lastly, the structural conformations of such proteins show greater conservation than do the corresponding amino acid sequences, as minor changes in protein sequence have minimal consequences on 3D structure.[47,48] Thus, our approach enables construction of a model of the 3D-structure of a target protein from its amino acid sequence by using, as template, the known 3D-structure of a related protein. The structure obtained from this homology modeling is considered to be one of the possible conformations of the target protein in its natural environment or at least, a very close approximation thereof. Thus, we used the published 3D crystal structure of JNK2 DFG-out as a template to resolve the 3D structures of JNK1 and JNK3 in their DFG-out conformations. The sequence homology rates between each target and the template were sizeable: ca. 80.562% for JNK2/JNK1 and ca. 76.724% for JNK2/JNK3. After completing model construction, the best models for JNK1 and JNK3 were identified using SWISS-MODEL software, which scores the options according to a linear combination of four statistical potential terms (beta interaction energy; all-atom pairwise energy; solvation energy; and torsion angle energy).[49] These models were then refined and validated (see below).

Model refinement. We first refined the models through energy minimization. Generally, this crucial step employs molecular mechanics and force fields to minimize the structure of the starting model and to remove any aberrant contacts or interactions within the 3D structure. Each model was uploaded into the Swiss-PdbViewer software,[50] in which the energy was minimized using the Energy-Minimization tool *in vacuo* (GROMOS96 43B1 parameters set without reaction field). The energy values for the minimized models were -21,206.189 KJ/mol for JNK1 and -21,205.189 KJ/mol for JNK3. This step afforded new 3D models of JNK1 and JNK3 in their DFG-out conformations, whose structures, as expected, are very close to that of JNK2 (Figure 2).

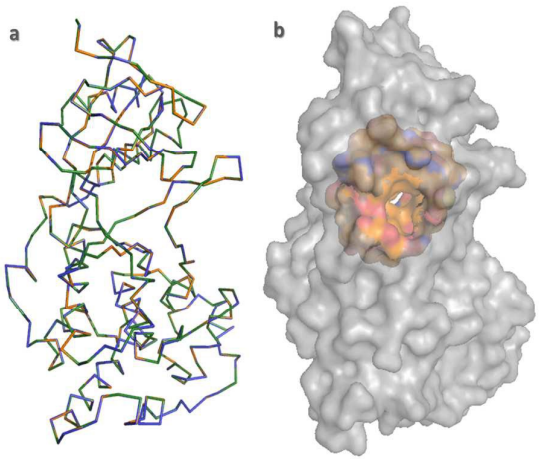

Figure 2 Structural alignment of the JNK1 and JNK3 DFG-out conformation models with the 3D X-ray structure of JNK2. (a) Backbone schematic representation, (b) Accessible surface area representation, in which the kinase active site pocket is highlighted in multicolor.

Model validation. The last step that we had to complete before being able to use the models was to validate the obtained 3D-structures. We began by validating the backbones and amino acid side-chain conformations for each model, by generating and analyzing the corresponding Ramachandran plots, which represent the distributions of the amino acid dihedral angles Phi and Psi (Figure 3). Each plot was obtained using the PROCHECK software package.[51] For the JNK1 model, 89% of the residues are in the most favored regions and 10%, in additional allowed regions, whereas 0.6% (two amino acids) are in disallowed regions. For the JNK3 model, 90% of the residues are in the most favored regions and 9.4%, in additional allowed regions, whereas 0.6% (two amino acids) are in disallowed regions. These results prove that the two models are highly plausible: indeed, for each model only two residues exhibit an exaggerated dihedral-angle torsion. Importantly, in each case these two amino acids are far from the active site; therefore, we reasoned that they should not influence our structural analysis.

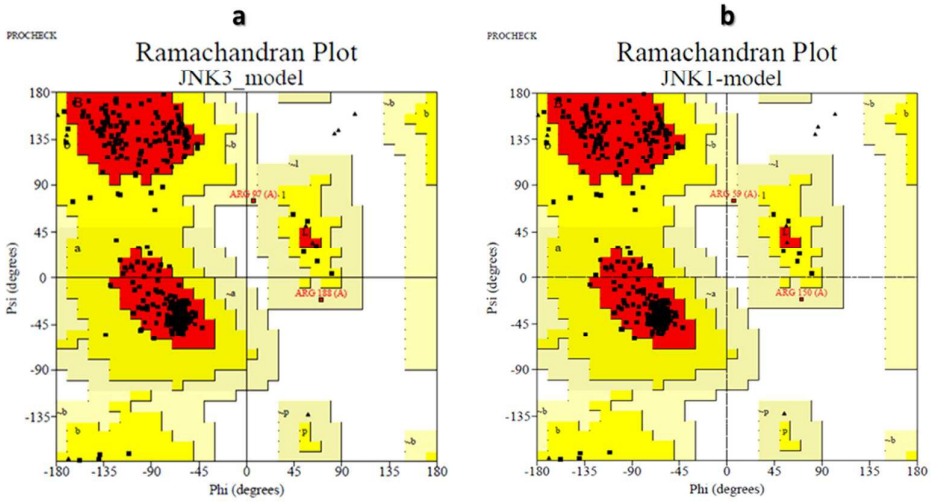

Figure 3 Ramachandran plots showing the distribution of the Phi and Psi dihedral angles of the amino acid side chains in the models of JNK3 (a) and JNK1 (b).

Next, we analyzed the statistics for the non-bonded interactions between different atom types in comparison with those from highly refined structures. For this analysis, we used ERRAT software.[52] The overall quality factors were *ca.* 95% for the JNK1 model and *ca.* 92% for the JNK3 model.

For the last structural validation step, we analyzed the compatibility of each atomic model (3D) with its amino acid sequence (1D), using Verify3D software. Each residue position in the 3D model is characterized by its environment and is represented by a row of 20 numbers in the profile. These numbers represent the statistical preference (called "3D-1D scores") of each of the 20 amino acids for this environment. The 3D profile score (S) for the compatibility of the sequence with the model is the sum of the 3D-1D scores over all residue positions for the amino acid sequence of the protein. For the two models, the percentage of residues with an average 3D-1D score of more than 0.2 was 93.28% for the JNK1 model and 90.76% for the JNK3 model. These scores demonstrated that the 3D structural models obtained are of high quality.

JNKs active sites analysis

Having refined and validated the models, we then sought to rationally design novel type-II JNK inhibitors, using structure-based drug design. To this end, we analyzed the active sites of each of the three JNKs, and then highlighted the sequences and the 3D residue-distribution of each site.

From the amino-acid sequence analysis (Figure 4), we aligned the three JNKs sequences by taking into account the gaps between residues. We found two sequence positions that differ by amino acid: Met-77 in JNK1, which corresponds to Leu-77 in JNK2 and to Met-115 in JNK3; and Ile-106 in JNK1, which corresponds to Leu-106 in JNK2 and to Leu-144 in JNK3. Although our sequence alignment highlighted some differences among the three active sites, we are currently unable to explain how such differences might influence the selectivity of certain kinase inhibitors (*e.g.* Birb796).

MedChemComm

ARTICLE

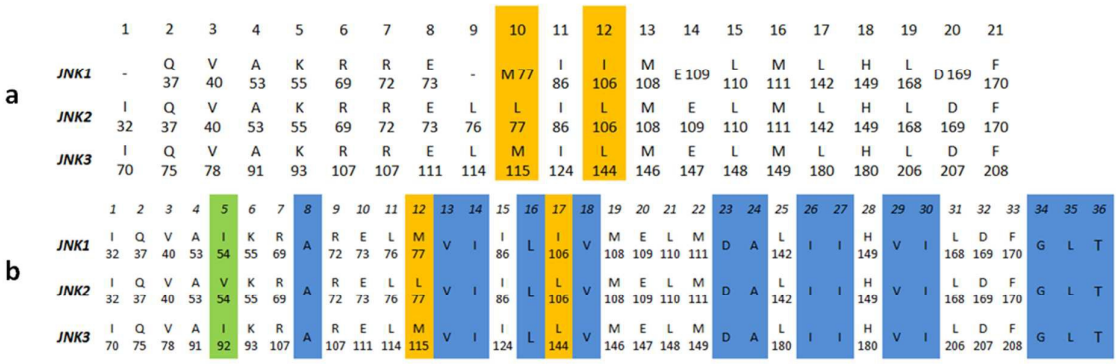

Figure 4 JNK DFG-out active-site sequence alignment. JNK DFG-out active-site sequences identified at a distance of **4Å** (**a**) or **6Å** (**b**) from Birb796. The gold columns highlight residue differences in corresponding positions; the blue columns, new residues involved in the active site construction at 6Å; and the green column, new different residues at 6Å.

Similarly to all enzymatic active sites in their natural state, kinase active-sites can adopt various forms and volumes, due chiefly to conformational changes in the A-loop and, to a lesser extent, to movement of amino acid side-chains. When kinases switch from the DFG-in conformation to the DFG-out conformation, the active site volume increases considerably – sometimes even doubling in size – as the newly formed DFG-out active-site pocket encompasses more residues. When extracting the complete sequence of the entire active site of a kinase in the context of inhibitor discovery, it is better to first consider the 3D-structure of the DFG-out conformation. Not only is each DFG-out active site larger than its corresponding DFG-in one, but more importantly, among the three JNKs, there is less sequence overlap among the DFG-out active sites than among the DFG-in ones, which translates to greater potential for ligand selectivity among the former than among the latter.

The X-ray structure of JNK2 in its DFG-out conformation co-crystallized with Birb796 reveals that the inhibitor occupies the entire active site. Specifically, the compound forms a complete "tunnel" that twists through the kinase, such that mapping of the JNK2 active site is representative of the entire kinase pocket. By using the mapping tool in Pymol Software, we selected all the residues within a given pocket size, defined as being either 4Å or 6Å from any atom of Birb796 in the 3D structure of JNK2 DFG-out. We considered that this set of amino acids, in their 3D rearrangement, forms the active site of the JNK2 DFG-out conformation. Since the homology models for JNK1 and JNK3 were obtained from the JNK2 template, we used the 3D alignment of the models with the 3D structure of JNK2/Birb796 as a reference to map the active sites of JNK1 and JNK3. As expected, sequence analysis of the mapped 3D active sites revealed very high similarity among the three JNKs, with the lowest identity percentage (85.71%) obtained at a 4Å shell for JNK1 versus JNK2 (Table 1).

Table 1 Identity percentages for DFG-out active-site sequence-alignments among JNK1, JNK2 and JNK3.

Pocket size	JNK1/JNK2	JNK1/JNK3	JNK2/JNK3	JNK1/JNK2/JNK3
Identity at 4Å	**85.71%**	**90.47%**	**95.23%**	**85.714%**
Identity at 6Å	**91.66%**	**97.22%**	**94.44%**	**90.789%**

Structure-based drug design analysis of the JNK2 DFG-out crystal structure aligned with the homology models obtained for JNK1 and JNK3 revealed that Birb796 into the JNK2 DFG-out active site fits very well, forming multiple interactions with the residues. Thus, we reasoned that such a good fit might explain the high selectivity of Birb796 for JNK2 (IC50: ~ 6 nM to 150 nM). On the other hand, when attempting to dock Birb796 into the JNK1 and JNK3 models, all the generated docking poses were outside the active sites and none was conclusive. These findings can explain the extremely low activity of Birb796 against these two kinases (IC50: > 10 000 nM for JNK1 ~ 1 400 nM for JNK3; *i.e.* more than tenfold less than against JNK2).

To study the lack of interaction between Birb796 and the DFG-out active site of either JNK1 or JNK3, we assessed the accessible surface of the active site of each of these JNKs with regards to possible positioning of Birb796. We compared the resulting values to that calculated for the active site of JNK2 (Figure 5).

MedChemComm

ARTICLE

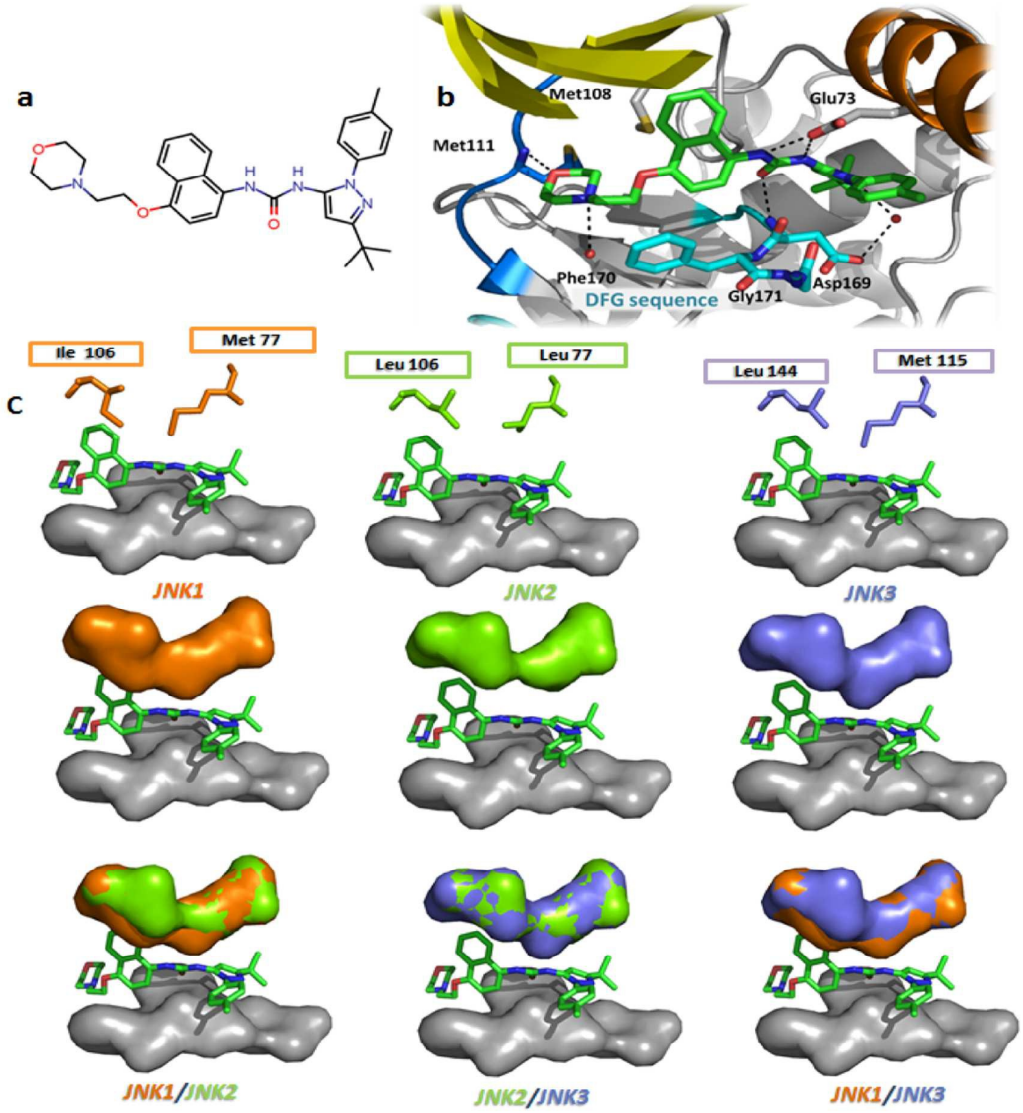

Figure 5 The Birb796 and the two sequence positions that differ by amino acid in the three JNK active sites. (**a**) Chemical structure of the Birb796, (**b**) The Birb796 (in green) in JNK2 active site (in gray) representation from 3NPC (in cyan the DFG sequence of JNK2) , (**c**) The two sequences positions sticks and surface representations

The two positions that represent the sequence differences among the three JNK members (position 1: JNK1-Met-77, JNK2-Leu-77 and JNK3-Met-115; and position 2: JNK1-Ile-106, JNK2-Leu-106 and JNK3-Leu-144) are located in the middle of the active-site roof (within the N-ter lobe of the kinase), and their side chains are oriented towards the active site. The residues in these two positions generate surfaces that influence the shape and volume of the active-site pockets. Relative to JNK2, in JNK3 the residues of these two positions generate a smaller pocket, thereby leaving less space for ligand binding. A similar, but even more pronounced, effect is seen in JNK1, in which the pocket is too small for ligand binding. The smaller volumes of the active sites in JNK1 and JNK3, relative to that of JNK2, are due mainly to the steric hindrance created at the two aforementioned positions.

Conclusion

Potent and selective kinase inhibitors are highly desirable for use as pharmacologic probes in interrogate kinase biology or as potential therapeutic agents. The JNK kinases, comprising JNK1, JNK2 and JNK3, are involved in diverse physiologic and pathologic processes, making them interesting targets for drug discovery in various indications. In the work reported here, we employed homology modeling to elucidate the 3D structure of JNK1 and JNK3 in their respective DFG-out conformations, as the only available structure for a JNK DFG-out conformation is that of JNK2 co-crystallized with the MAPK inhibitor Birb796. We found a high degree of structural similarity among the three members, which might partly explain why certain JNK inhibitors lack selectivity towards any one of the three members. Using structure-based drug design, and the known inhibitor Bibr796, we have analyzed the structural differences among the three JNKs in terms of their respective active site pockets. Specifically, we have identified two critical positions in the active site that differ by amino acid among the three JNKs. The steric hindrance created by these residues in JNK1 and JNK3, and the physico-chemical properties of these enzymes, help explain the selectivity of Birb796 for JNK2. These findings opened new insights into the rational design of novel compounds for selective manipulation of JNKs.

Acknowledgements

This research was supported by the PHC PROGRAM WITH MOROCCO, French agency for the promotion of higher education, hospitality and international mobility.

References

1 M. A. Fabian, W. H. Biggs, D. K. Treiber, C. E. Atteridge, M. D. Azimioara, M. G. Benedetti, T. A. Carter, P. Ciceri, P. T. Edeen, M. Floyd, J. M. Ford, M. Galvin, J. L. Gerlach, R. M. Grotzfeld, S. Herrgard, D. E. Insko, M. A. Insko, A. G. Lai, J.-M. Lélias, S. A. Mehta, Z. V. Milanov, A. M. Velasco, L. M. Wodicka, H. K. Patel, P. P. Zarrinkar and D. J. Lockhart, *Nat. Biotechnol.*, 2005, **23**, 329–336.
2 J. Zhang, P. L. Yang and N. S. Gray, *Nat. Rev. Cancer*, 2009, **9**, 28–39.
3 Y. Landry and J.-P. Gies, *Fundam. Clin. Pharmacol.*, 2008, **22**, 1–18.
4 R. J. Davis, *Cell*, 2000, **103**, 239–252.
5 S. Gupta, T. Barrett, A. J. Whitmarsh, J. Cavanagh, H. K. Sluss, B. Derijard and R. J. Davis, *EMBO J.*, 1996, **15**, 2760–2770.
6 B. Dérijard, M. Hibi, I.-H. Wu, T. Barrett, B. Su, T. Deng, M. Karin and R. J. Davis, *Cell*, 1994, **76**, 1025–1037.
7 T. Kallunki, B. Su, I. Tsigelny, H. K. Sluss, B. Dérijard, G. Moore, R. Davis and M. Karin, *Genes Dev.*, 1994, **8**, 2996–3007.
8 H. K. Sluss, T. Barrett, B. Dérijard and R. J. Davis, *Mol. Cell. Biol.*, 1994, **14**, 8376–8384.
9 A. A. Mohit, J. H. Martin and C. A. Miller, *Neuron*, 1995, **14**, 67–78.
10 R. K. Barr and M. A. Bogoyevitch, *Int. J. Biochem. Cell Biol.*, 2001, **33**, 1047–1063.
11 C. R. Weston and R. J. Davis, *Curr. Opin. Cell Biol.*, 2007, **19**, 142–149.
12 L. Chang and M. Karin, *Nature*, 2001, **410**, 37–40.
13 A. Lin, *BioEssays News Rev. Mol. Cell. Dev. Biol.*, 2003, **25**, 17–24.
14 M. Karin, *J. Biol. Chem.*, 1995, **270**, 16483–16486.
15 K. Yamamoto, H. Ichijo and S. J. Korsmeyer, *Mol. Cell. Biol.*, 1999, **19**, 8469–8478.
16 K. Maundrell, B. Antonsson, E. Magnenat, M. Camps, M. Muda, C. Chabert, C. Gillieron, U. Boschert, E. Vial-Knecht, J.-C. Martinou and S. Arkinstall, *J. Biol. Chem.*, 1997, **272**, 25238–25242.
17 C. Yu, Y. Minemoto, J. Zhang, J. Liu, F. Tang, T. N. Bui, J. Xiang and A. Lin, *Mol. Cell*, 2004, **13**, 329–340.
18 E. F. Wagner and A. R. Nebreda, *Nat. Rev. Cancer*, 2009, **9**, 537–549.
19 A. Gdalyahu, I. Ghosh, T. Levy, T. Sapir, S. Sapoznik, Y. Fishler, D. Azoulai and O. Reiner, *EMBO J.*, 2004, **23**, 823–832.
20 M. Gao, T. Labuda, Y. Xia, E. Gallagher, D. Fang, Y.-C. Liu and M. Karin, *Science*, 2004, **306**, 271–275.
21 A. M. Manning and R. J. Davis, *Nat. Rev. Drug Discov.*, 2003, **2**, 554–565.
22 H. Okazawa and S. Estus, *Am. J. Alzheimers Dis. Other Demen.*, 2002, **17**, 79–88.
23 Z. Han, D. L. Boyle, K. R. Aupperle, B. Bennett, A. M. Manning and G. S. Firestein, *J. Pharmacol. Exp. Ther.*, 1999, **291**, 124–130.
24 Z. Han, D. L. Boyle, L. Chang, B. Bennett, M. Karin, L. Yang, A. M. Manning and G. S. Firestein, *J. Clin. Invest.*, 2001, **108**, 73–81.
25 P. R. Eynott, P. Nath, S.-Y. Leung, I. M. Adcock, B. L. Bennett and K. F. Chung, *Br. J. Pharmacol.*, 2003, **140**, 1373–1380.
26 P. R. Eynott, L. Xu, B. L. Bennett, A. Noble, S.-Y. Leung, P. Nath, D. A. Groneberg, I. M. Adcock and K. F. Chung, *Immunology*, 2004, **112**, 446–453.
27 P. Nath, P. Eynott, S.-Y. Leung, I. M. Adcock, B. L. Bennett and K. F. Chung, *Eur. J. Pharmacol.*, 2005, **506**, 273–283.
28 R. Ricci, G. Sumara, I. Sumara, I. Rozenberg, M. Kurrer, A. Akhmedov, M. Hersberger, U. Eriksson, F. R. Eberli, B. Becher, J. Borén, M. Chen, M. I. Cybulsky, K. J. Moore, M. W. Freeman, E. F. Wagner, C. M. Matter and T. F. Lüscher, *Science*, 2004, **306**, 1558–1561.
29 N. J. Kennedy and R. J. Davis, *Cell Cycle Georget. Tex*, 2003, **2**, 199–201.
30 J. Hirosumi, G. Tuncman, L. Chang, C. Z. Görgün, K. T. Uysal, K. Maeda, M. Karin and G. S. Hotamisligil, *Nature*, 2002, **420**, 333–336.
31 A. Jaeschke, M. Rincón, B. Doran, J. Reilly, D. Neuberg, D. L. Greiner, L. D. Shultz, A. A. Rossini, R. A. Flavell and R. J. Davis, *Proc. Natl. Acad. Sci. U. S. A.*, 2005, **102**, 6931–6935.
32 Q. Liang and J. D. Molkentin, *J. Mol. Cell. Cardiol.*, 2003, **35**, 1385–1394.
33 S. Hunot, M. Vila, P. Teismann, R. J. Davis, E. C. Hirsch, S. Przedborski, P. Rakic and R. A. Flavell, *Proc. Natl. Acad. Sci. U. S. A.*, 2004, **101**, 665–670.
34 J. Peng and J. Andersen, *IUBMB Life*, 2003, **55**, 267–271.
35 H. M. Berman, J. Westbrook, Z. Feng, G. Gilliland, T. N. Bhat, H. Weissig, I. N. Shindyalov and P. E. Bourne, *Nucleic Acids Res.*, 2000, **28**, 235–242.
36 T. U. Consortium, *Nucleic Acids Res.*, 2014, **42**, D191–D198.
37 F. Sievers, A. Wilm, D. Dineen, T. J. Gibson, K. Karplus, W. Li, R. Lopez, H. McWilliam, M. Remmert, J. Soding, J. D. Thompson and D. G. Higgins, *Mol. Syst. Biol.*, 2014, **7**, 539–539.
38 K. Arnold, L. Bordoli, J. Kopp and T. Schwede, *Bioinformatics*, 2006, **22**, 195–201.
39 T. Schwede, J. Kopp, N. Guex and M. C. Peitsch, *Nucleic Acids Res.*, 2003, **31**, 3381–3385.
40 R. A. Laskowski, M. W. MacArthur, D. S. Moss and J. M. Thornton, *J. Appl. Crystallogr.*, 1993, **26**, 283–291.
41 A. Kuglstatter, M. Ghate, S. Tsing, A. G. Villaseñor, D. Shaw, J. W. Barnett and M. F. Browner, *Bioorg. Med. Chem. Lett.*, 2010, **20**, 5217–5220.
42 O. Trott and A. J. Olson, *J. Comput. Chem.*, 2010, **31**, 455–461.
43 *The PyMol Molecular Graphics System, Version 0.99rc6, Schrodinger, LLC*, .
44 C. Chothia and A. M. Lesk, *EMBO J.*, 1986, **5**, 823–826.
45 S. Kaczanowski and P. Zielenkiewicz, *Theor. Chem. Acc.*, 2010, **125**, 643–650.
46 V. K. Vyas, R. D. Ukawala, M. Ghate and C. Chintha, *Indian J. Pharm. Sci.*, 2012, **74**, 1–17.
47 J.-M. Chandonia and S. E. Brenner, *Proteins*, 2005, **58**, 166–179.
48 D. Vitkup, E. Melamud, J. Moult and C. Sander, *Nat. Struct. Biol.*, 2001, **8**, 559–566.
49 P. Benkert, M. Biasini and T. Schwede, *Bioinformatics*, 2011, **27**, 343–350.
50 M. U. Johansson, V. Zoete, O. Michielin and N. Guex, *BMC Bioinformatics*, 2012, **13**, 173.
51 R. A. Laskowski, M. W. MacArthur, D. S. Moss and J. M. Thornton, *J. Appl. Crystallogr.*, 1993, **26**, 283–291.

52 C. Colovos and T. O. Yeates, *Protein Sci. Publ. Protein Soc.*, 1993, **2**, 1511–1519.